Mechanical Properties of Copper Micrometer Pillars Fabricated by Intermittent MAGE Process

J. C. Lin[1,2,], Y. S. Chen[2], C. F. Huang[2], J. H. Yang[2], T. K. Chang[2], Chung-Lin Wu[3],*
Y. R. Hwang[2], T. C. Chen[2]

[1] Institute of Materials Science and Engineering, Central University, No.300, Jhongda Rd., Jhongli City, Taoyuan County 320, Taiwan, R.O.C
[2] Department of Mechanical Engineering, National Central University, No.300, Jhongda Rd., Jhongli City, Taoyuan County 320, Taiwan, R.O.C
[3] Center for Measurement Standards, Industrial Technology Research Institute, Hsinchu 30011 Taiwan, R.O.C
[*]E-mail: jclincom@cc.ncu.edu.tw

A nano-universal testing machine (Nano-UTM) was used to investigate the mechanical properties of micrometer-sized copper pillars fabricated by the intermittent microanode guided electrodeposition (MAGE) process under various voltages (i.e., 2.8–3.0 V) and initial gaps (5–15 μm) between the electrodes. The Young's modulus, yield strength, fracture strength, and strain were deduced from the testing data, and their magnitudes were determined for the experimental conditions used with MAGE. The mechanical strength was higher for micropillars that were fabricated at lower voltages with greater initial separation (e.g., with the voltage at 2.8 V and initial gap at 15 μm) than those fabricated at higher voltages with smaller initial separation (e.g., with the voltage at 3.0 V and initial gap at 5 μm). After examining the surface morphology and transverse microstructure, we found that the stronger pillars revealed a smooth appearance with a dense internal microstructure, whereas the weaker pillars revealed a rough appearance with a porous internal microstructure. The fracture morphology was investigated to clarify the failure mechanism for various micrometer-sized copper pillars fabricated using the same MAGE process but under different conditions.

1. INTRODUCTION

In 1995, Hunter et al. [1,2] exploited the innovative technology of localized electrochemical deposition (LECD) to fabricate three-dimensional metallic microfeatures. This technique avoids the

need for expensive equipment and special facilities such as a cleanroom to make the manufacture of metallic micrometer-sized structures in ordinary laboratories possible. Recently, progress in the development of microelectromechanical systems (MEMS) has drawn attention to the use of the LECD process to manufacture micro-components or devices. El-Giar et al. [3,4] carried out the LECD process to construct a micrometer-sized copper wire that can be used as an interconnector in microelectronic devices. Said et al. [5,6] fabricated several copper microstructures by means of LECD and discussed the dependence of their surface morphology on the deposition rate. Seol et al. [7–9] used coherent microradiology to look into the in situ development in the local region during localized electrochemical deposition. Based on their results, they proposed a qualitative model to demonstrate the growth and formation of micrometer-sized copper columns via the migration and diffusion of copper ions in the electrochemical process. This radiographic technique also provides a good tool for examining the growth and development of a hollow micrometer-sized copper tube fabricated by LECD. Yeo et al. [10] investigated the fabrication of nickel micro-columns by LECD and concluded that their surface morphology is significantly influenced by the size and geometry of the microanode.
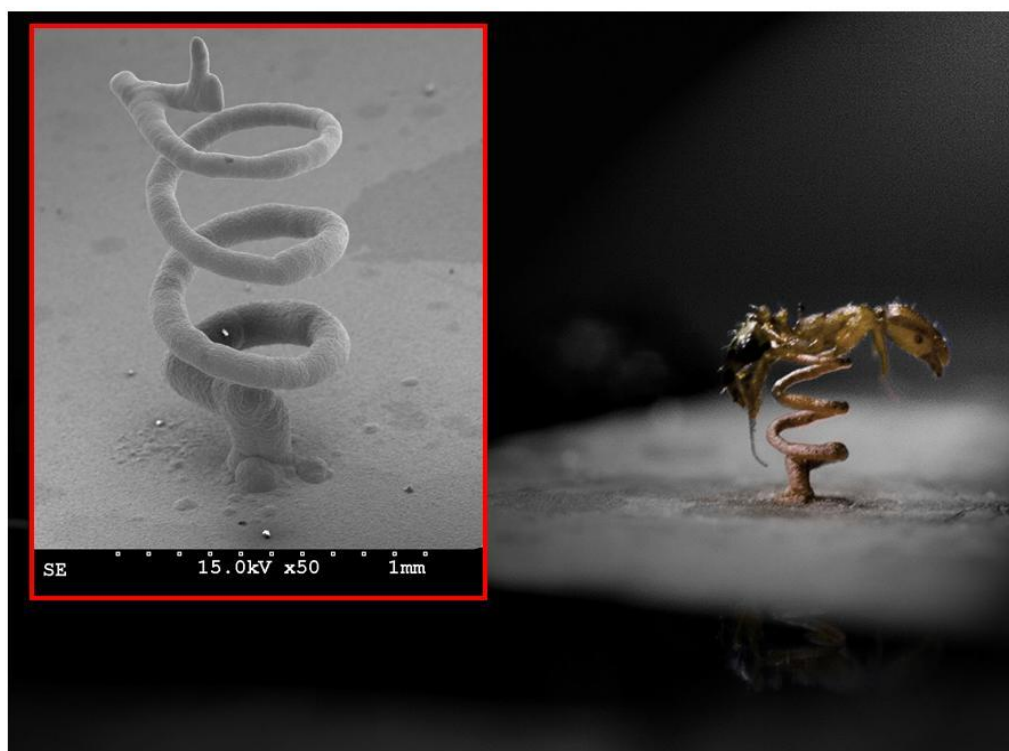

Figure 1. Optical micrograph for a micrometer-sized copper spring fabricated by intermittent MAGE with an ant put on the top for comparison purposes.

In our earlier work [11], we developed a system in which a microanode can be controlled to move in continuous or intermittent mode during LECD. Because of this, we termed the LECD process in a rather explicit manner (i.e., microanode guided electroplating (MAGE)) to acknowledge that electrochemical deposition only proceeds to the local region that is pointed at initially by the tip of the

microanode and follows the track guided by the microanode. Based on real-time measurement of the current for MAGE with intermittent motion of the microanode at constant voltages, we published several works [12–17] aimed towards realizing the LECD mechanism by proposing models that dealt with the balance of mass transport between the location undergoing LECD and its peripheral bulk solution. In an attempt to construct three-dimensional metallic microfeatures by LECD, we made strenuous efforts to design hardware and software for the motion control of the microanode and finally fabricated a micrometer-sized copper spring via MAGE. Figure 1 depicts the optical micrograph of a micrometer-sized copper spring fabricated by intermittent MAGE. The deposition was performed in a 0.5 M copper sulfate solution; a platinum microanode (diameter of 125 μm) was used to guide the deposition at a voltage of2.8 V and initial gap of 10 μm between the electrodes. An ant was put on the top of this microspring to compare their sizes. The inset displays the scanning electron microscopy (SEM) image of this spring, which was approximately 1 mm in height and 500 μm in diameter. The diameter of the copper was about 50 μm on the spring top but tended to be more (60–80 μm) from top to bottom.

There have been few reports and little discussion on the mechanical properties of micro-pillars fabricated by the LECD process. Lin et al. [18] studied the Young's modulus of micrometer-sized copper pillars indirectly. They found that the modulus is significantly influenced by defects that possibly arise from improper control of the experimental conditions. In the present study, we investigated the mechanical properties of copper micro-pillars in a direct manner (i.e., by employing a micro-tensile tester). By examining the fracture morphology, we also tried to establish a mechanism to illustrate the tensile behavior of micropillars fabricated under various conditions.

2. EXPERIMENTAL DETAILS

Specimens of micrometer-sized copper pillars were prepared by the localized electrochemical deposition process (LECD) from a bath of 0.5 M copper sulfate under a variety of experimental conditions. LECD was carried out by microanode guided electroplating (MAGE) in which a piece of Pt wire (125 m in diameter) acted as a microanode to guide the electroplating. One end of the Pt wire was welded with copper conducting wire.

The Cu-welded Pt wire was fixed coaxially by a Bakelite tube (0.5 mm in diameter and 60 mm in length) and cold-mounted with epoxy resin. The Pt end of the cylinder was ground with 400-grit emery paper to expose the tip to air. The exposed tip was further ground with a sequence of emery papers up to 1200 grit and then polished with 3.0 and 0.5 μm Al_2O_3 powders to form a smooth disk (125 μm in diameter) for use as a microanode when the copper conducting wire was connected with the positive pole of a dc power supply during MAGE.

Prior to electroplating, the microanode was kept in contact with the cathode, which was a square (10 mm × 10 mm × 1 mm) of pure copper (99.9 wt.%) that was mounted with epoxy resin. The front surface was ground by a sequence of emery papers (grades 600–1200) and wet-polished with 0.5 μm Al_2O_3 powders for a mirror surface.
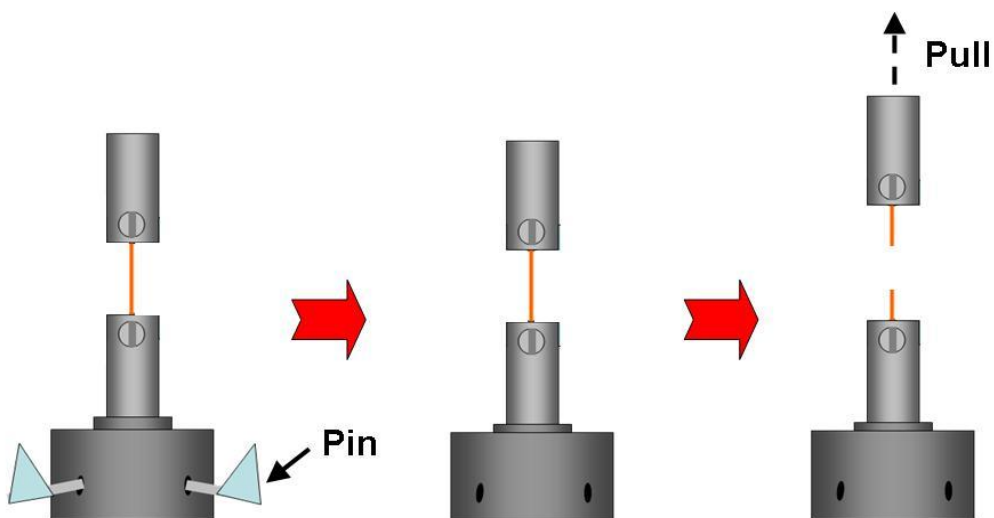
Figure 2. Schematic setup of the Nano-UTM with the specimens for the mechanical test.
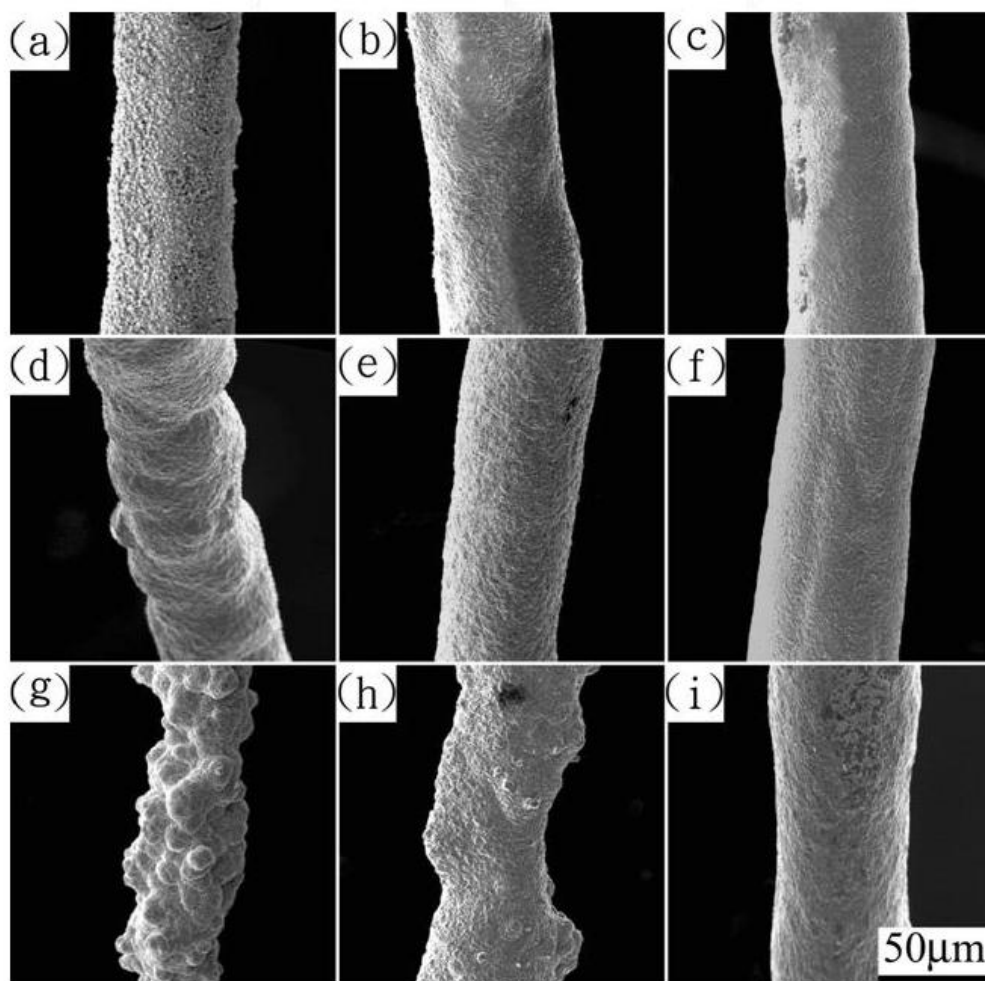

Figure 3. Secondary electron micrographs (SEM) of the copper micro-pillars fabricated by MAGE in a 0.5 M copper sulfate solution with the following electric voltages and initial gaps between the electrodes: (a) 2.8 V, 5 μm; (b) 2.8 V, 10 μm; (c) 2.8 V, 15 μm; (d) 2.9 V, 5 μm; (e) 2.9 V, 10 μm; (f) 2.9 V, 15 μm; (g) 3.0 V, 5 μm; (h) 3.0 V, 10 μm; (i) 3.0 V, 15 μm.

An electrolyte cell (35 mm × 35 mm × 90 mm) made of polymethyl methacrylate (PMMA) was filled with 1×10^{-4} m^3 freshly prepared solution containing 0.5 M CuSO$_4$·5H$_2$O and 0.5 M H$_2$SO$_4$ that was ready for MAGE.

The experimental setup and intermittent MAGE process were reported in our previous work [11]. Prior to MAGE, the microanode was first placed in contact with the cathode substrate and withdrawn to keep an initial separation of 5, 10, and 15μm from the cathode before the start of electroplating. The electrical voltages between the electrodes were controlled to be 2.8, 2.85, 2.9, 2.95, and 3.0 V during the MAGE process.

A nano-universal testing machine (Nano-UTM, Surface & Surface System & Technology GmbH & CO., Germany) was employed for the mechanical tests of the copper micro-pillars. The testing data were recorded and processed with a personal computer, and the results were reported as a plot of the engineering stress against the engineering strain.

The micro-pillars were prepared by intermittent MAGE to a length of 2 mm and removed from the copper substrate with a clip. The ends of the micro-pillar on the sheet were tightly held by the screws, and the pins were removed. A constant strain rate of 0.001 mm/s was applied in the test. Figure 2 is a schematic setup of the Nano-UTM with the specimen used in the micro-tensile test. The fracture surface of the broken specimens was examined through scanning electron microscopy (SEM, Hitachi, S-3500N, Japan).

3. RESULTS

3.1. SEM surface morphologies for the micropillars prior to and post UTM testing

Fig. 3 depicts the SEM morphologies for the micrometer-sized copper pillars fabricated by the MAGE process under various experimental conditions. The electrical voltages were set at 2.8 V (Figs. 3(a)–(c)), 2.9 V (Figs. 3(d)–(f)), and 3.0 V (Figs. 3(g)–(i)). The initial separations between the electrodes were 5 μm (Figs. 3(a), (d), and (g)), 10 μm (Figs. 3(b), (e), and (h)), and 15 μm (Figs. 3(c), (f), and (i)).

All of the copper micro-pillars shown in Fig. 3 seemed to reveal a diameter of roughly 75 μm. However, the pillars revealed different diameters and distinctive appearances depending upon the electrical voltage and initial gap employed between the electrodes in MAGE. When comparing the micrographs in Fig. 3(a) with Figs. 3(b) and (c), the micro-pillars fabricated at 2.8 V exhibited a uniform diameter and smoother surface comprised of finer particles when the initial gap was increased from 5 μm to 10 μm and even more so at 15 μm. In other words, pillars prepared at a higher initial gap produced a smoother surface and uniform diameter.

On the other hand, when the initial gap was fixed at constant separation (i.e., 5, 10, or 15 μm) and MAGE was performed at increasing voltages of 2.8, 2.9, and 3.0 V, the micro-pillars had diameters that were less uniform (Figs. 3(a), (d), and (g); Figs. 3(b), (e), and (h)) and rougher surfaces (Figs. 3(c), (f), and (i). The variation in SEM morphologies shown in Fig. 3 is discussed later in Section 4.
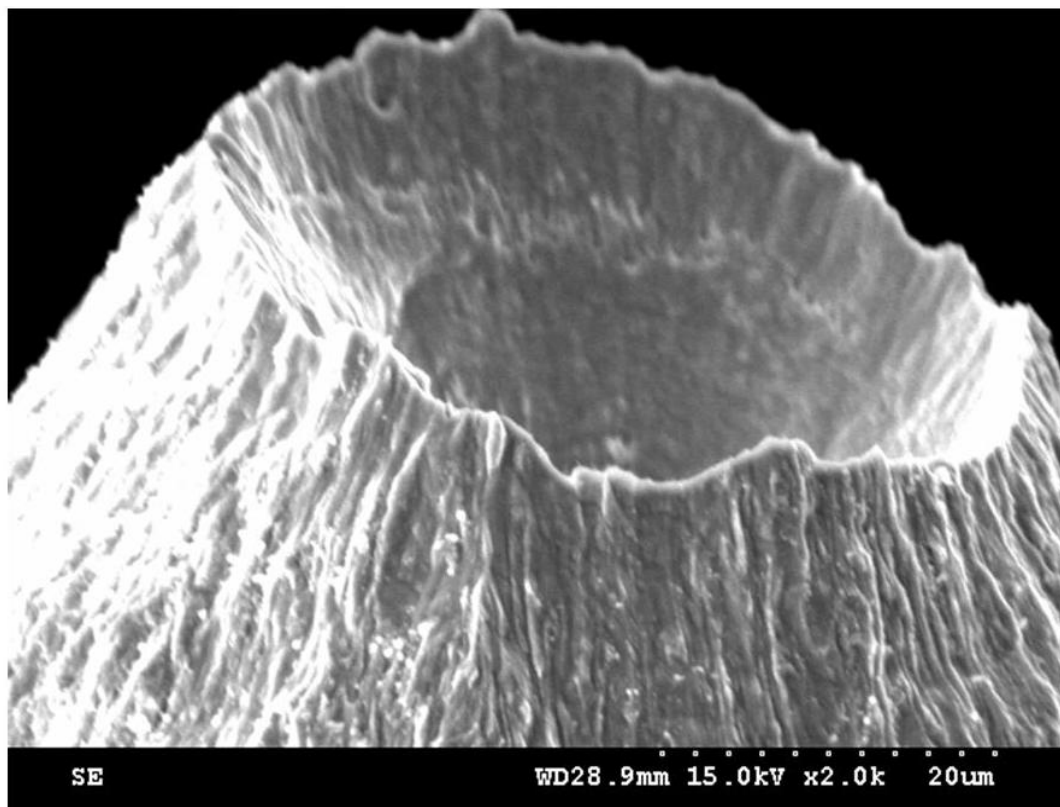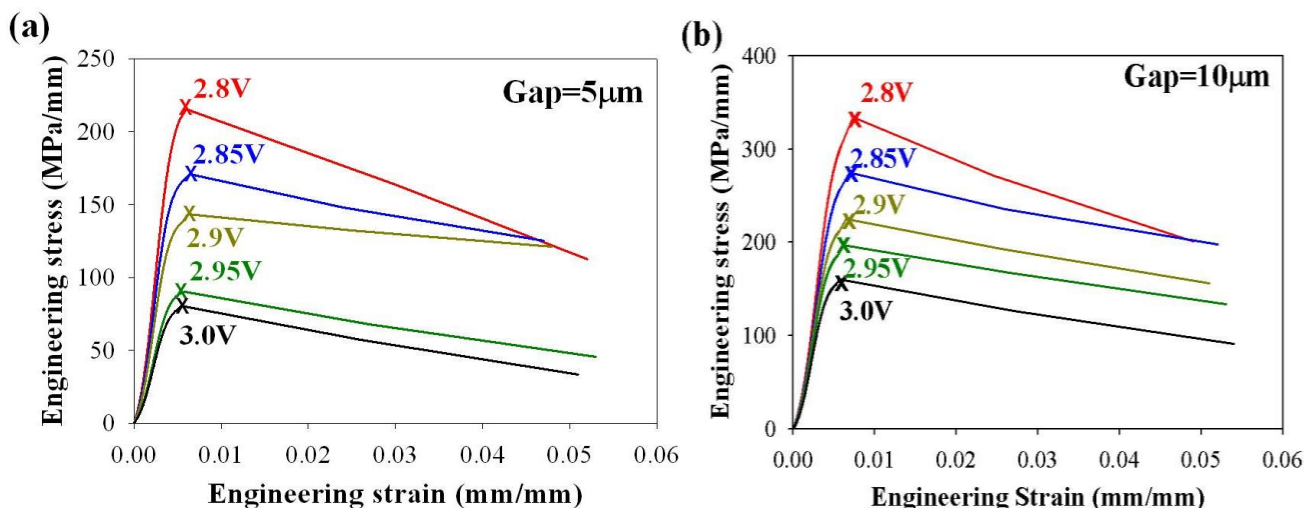
Figure 4. Plots of the stress against strain in response to micro-tensile testing of the copper micro-pillars fabricated in 0.5 M copper sulfate solution by intermittent MAGE under voltages of 2.85–3.00 V with initial gaps between the electrodes of (a) 5 μm, (b) 10 μm, and (c)15 μm.

Figure 4 presents the SEM morphology for one of the fracture surfaces after tensile testing by Nano-UTM for a specimen fabricated at 3.0 V with an initial gap of 5 μm. The fracture surface revealed a cup and cone morphology that was predominantly brittle with somewhat tensile characteristics. Fig. 4 reveals the deep volcanic surface of the broken cup component with necking around the periphery of the fracture.
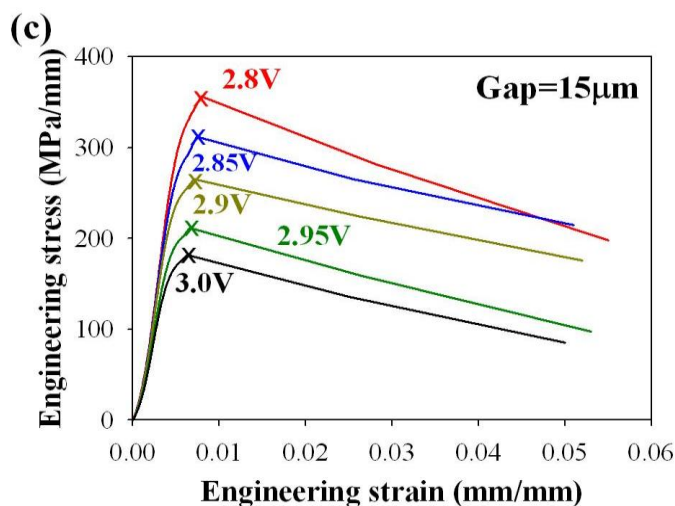
(c)

Figure 5. Schematic derivation of Young's modulus, yield strength, fracture stress, and fracture strain from a typical plot of stress-strain recorded during the micro-tensile test of the copper micropillars.

3.2. Stress-stain curves obtained from the tests by Nano-UTM

Figures 5 (a)–(c) indicate the stress-strain curves that resulted from testing by the Nano-UTM at a constant strain rate of 0.001 mm/s for the micrometer-sized copper pillars fabricated by intermittent MAGE under various voltages and initial gaps. Figure 5(a) displays the plots of engineering stress against engineering strain for the copper micro-pillars electrochemically fabricated at an initial gap of 5 μm but with various voltages (i.e., 2.80, 2.85, 2.90, 2.95, and 3.00 V). Figures 5(b) and (c) exhibit similar plots for micro-pillars fabricated using the same voltages but with initial gaps of 10 and 15 μm, respectively.

All of the plots started with linear regions through the zero point. They turned into curves, reached the maxima, and suddenly ended with fracture. In Figs. 5(a)–(c), the micro-pillars clearly depict higher stress when they were fabricated under lower voltages (e.g., at 2.80 and 2.85 V) irrespective of the magnitudes of the initial gap. When comparing micro-pillars fabricated at a constant voltage (e.g., 2.80 V), the pillars fabricated at the lowest initial gap (i.e., 5 μm in Fig. 5 (a)) revealed the weakest stress; those fabricated with the medium gap (i.e., 10 μm in Fig. 5(b)) displayed the medium stress; and those fabricated with the greatest gap (i.e., 15 μm in Fig. 5 (c)) exhibited the strongest stress.

In other words, the strength for the micro-pillars decreased with increasing voltage for a constant initial gap; however, the strength increased with increasing initial gap when MAGE was performed at a constant voltage.

This plot of stress against strain defines the elastic and plastic deformation, yield, and tensile and fracture strength well. We checked the plots depicted in Fig. 5 to determine the yield strength for all of the copper micro-pillars fabricated in this work. To estimate the mechanical properties of the pillars, we try to define the terms in the following sections and discuss them in detail.
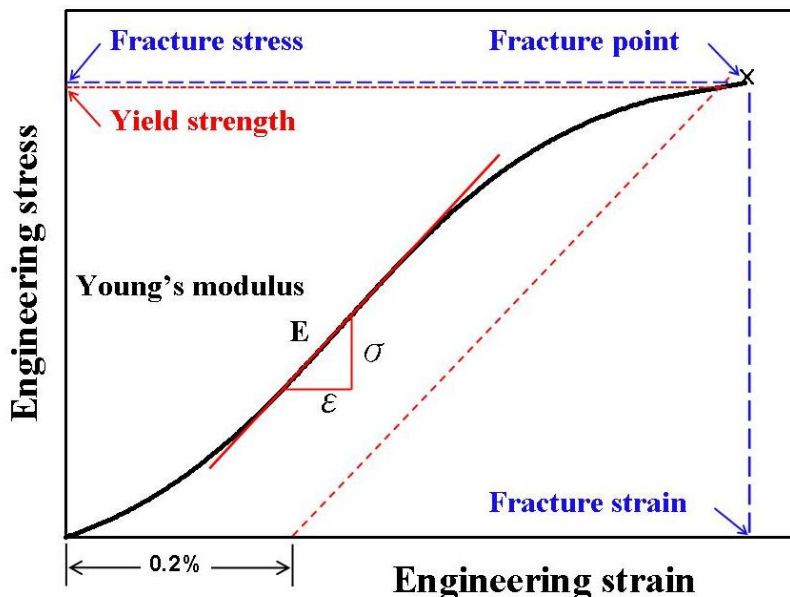
Figure 6. Data of Young's modulus for the copper micro-pillars fabricated by MAGE as a function of the electric voltages employed in MAGE for different gaps between the electrodes.

4. DISCUSSION

4.1. Mechanical properties estimated from the plots of stress versus strain

Figure 6 displays a schematic estimation for mechanical properties such as the Young's modulus, yield strength, fracture stress, and fracture strain from a general curve plotted in the diagram of the engineering stress versus engineering strain as depicted in Fig. 5.
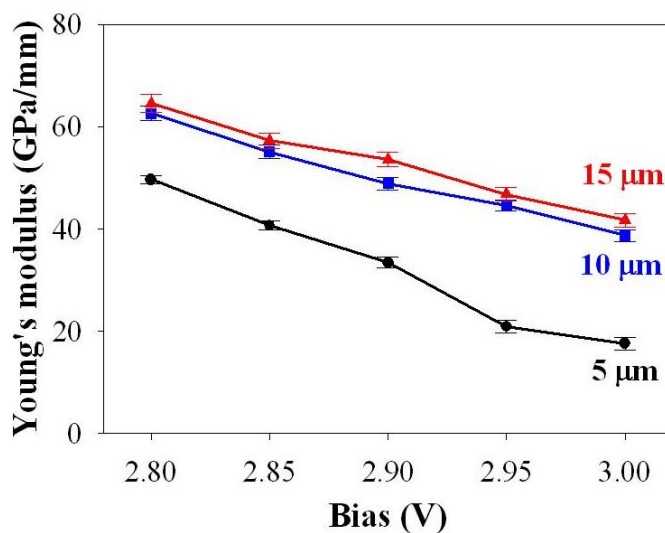

Figure 7. Data of yield strength for the copper micro-pillars fabricated by MAGE as a function of the electric voltages employed in MAGE for different gaps between the electrodes.

Young's modulus was estimated from the slope of the line region that was fitted to reveal the best superpose with the curve. A 0.2% strain offset line was constructed to intersect with the stress-strain curve. The stress in response to the intersection was defined as the yield strength (offset yield strength method). The stress at the fracture point was defined as the fracture stress, and its corresponding strain was the fracture strain. The plots in Figs. 5(a)–(c) were treated the same way as that in Fig. 6 to estimate the mechanical properties. The data results for the Young's modulus, yield strength, and fracture stress and fracture strain are shown in Figs. 7, 8, and 9, respectively.
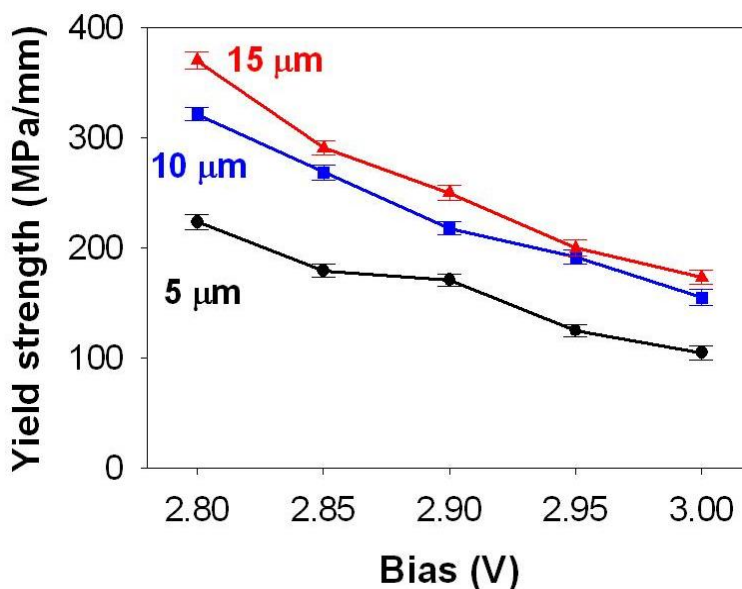

Figure 8. Dependence of the (a) fracture stress and (b) fracture strain for the copper micro-pillars fabricated by MAGE on the electric voltage for different initial gaps between electrodes.

In Fig. 7, the copper micro-pillars revealed that their Young's modulus depends upon the voltages and gaps employed in MAGE. At a constant gap of 5 μm, the Young's modulus decreased from 49.7 GPa/mm to 17.6 GPa/mm when the voltage was increased from 2.8 V to 3.0 V. On the other hand, at a constant voltage of 2.8 V, the Young's modulus increased from 49.7 GPa/mm to 64.6 GPa/mm when the gap was increased from 5 μm to 15 μm. This implies that the copper micro-pillars fabricated under a lower electric field (2.8 V with an initial gap of 15 μm) are much stronger (about 3.67 times) at resisting elastic deformation than those fabricated under a higher electric field (3.0 V with an initial gap of 5 μm).

Figure 8 demonstrates the dependence of the yield strength upon the voltages and initial gaps employed in MAGE to fabricate the copper micro-pillars. For the micro-pillars fabricated at a constant voltage (i.e., 3.0 V), the yield strength increased from 104.90 MPa/mm to 173.44 MPa/mm when the gap was increased from 5 μm to 15 μm. For the pillars fabricated at a constant gap of 15 μm, the yield strength decreased from 370.31 MPa/mm to 173.44 MPa/mm when the voltage was increased from 2.8 V to 3.0 V. Since the yield strength is the critical stress at which plastic deformation occurs, it plays an important role in the manufacturing of metallic materials**.** The copper micro-pillars fabricated by

MAGE under the lowest electric field (2.8 V with an initial gap of 15 μm) were more resistant (about 3.53 times) to plastic deformation than those fabricated under the highest electric field (3.0 V with an initial gap of 5 μm).

Figure 9 depicts the dependence of (a) fracture stress and (b) fracture strain upon the voltages employed to fabricate the copper micro-pillars by MAGE under different initial gaps. When the voltage was set at 3.0 V in MAGE, the fabricated micro-pillars increased their fracture stress from 80.63 MPa to 181.45 MPa when the initial gap was increased from 5 μm to 15 μm; the fracture strain increased from 0.0054 mm/mm to 0.0063 mm/mm. When a constant initial gap at 15 μm was set in MAGE, the fabricated micro-pillars decreased their fracture stress from 356.18 MPa to 181.45 MPa when the voltage was increased from 2.8 V to 3.0 V; the fracture strain also decreased from 0.0079 mm/mm to 0.0063 mm/mm. In terms of electric field strength, the copper micro-pillars fabricated by MAGE in the lowest field (2.8 V with an initial gap of 15 μm) had much stronger (about 4.42 times) fracture strength than those fabricated in the highest field (3.0 V with an initial gap of 5 μm). Moreover, the copper pillars fabricated in the lowest field displayed greater (roughly 1.46 times) fracture strain than those fabricated in the highest field.
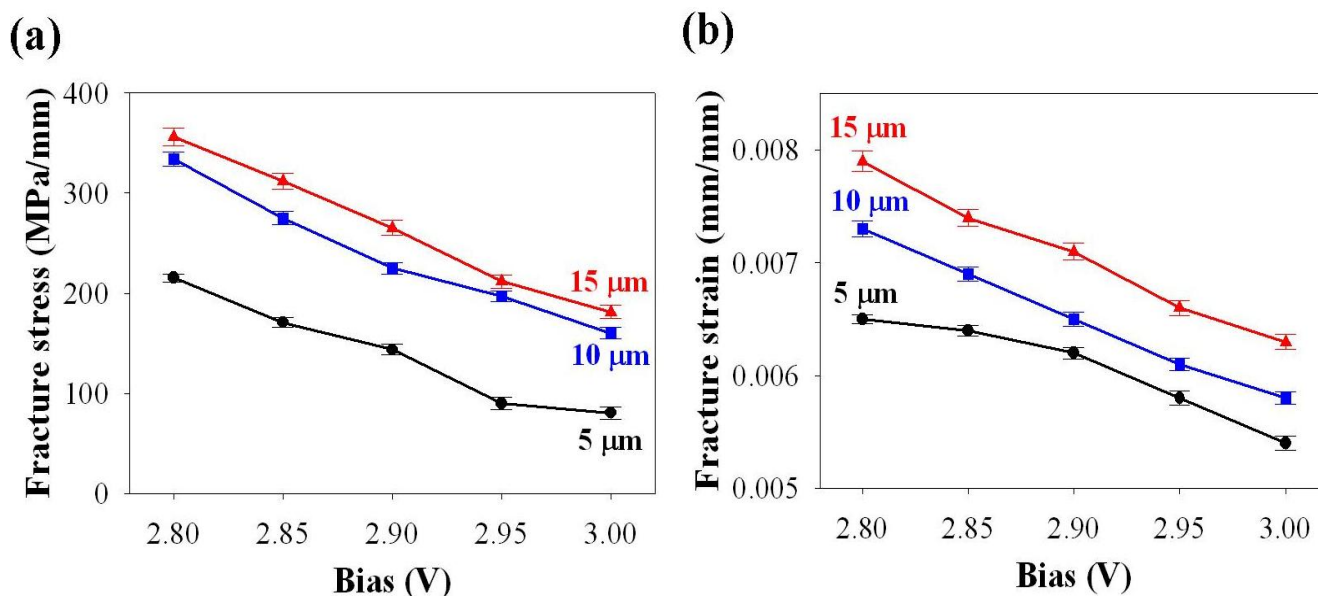

Figure 9. Data of resilience modulus for the copper micro-pillars as a function of electric voltages for different initial gaps employed in the MAGE process.

4.2. Internal microstructures of copper micropillars fabricated under two extreme conditions

The mechanical properties of the copper micro-pillars are believed to depend upon their internal microstructures, which are significantly determined by the experimental conditions in the MAGE process. Scanning electron microscopy (SEM) was used to examine the internal microstructure for the cross-section of the copper pillars. Figure 10 depicts the cross-sectional SEM morphologies of the copper micro-pillars fabricated under two extreme conditions: i.e., the lowest (Fig. 10(a)) and highest

electric fields (Fig. 10(b)). The cross-sectional morphology in Fig. 10(a) revealed a dense internal microstructure for the pillar fabricated at 2.8 V with an initial gap of 15μm. In contrast, the cross-sectional SEM morphology in Fig. 10(b) displayed an internal microstructure that was less dense and contained few defects for the pillar fabricated at 3.0 V with an initial gap of 5 μm. The interior of the copper micro-pillar seemed to be constructed in U-shape curved layers with few voids. The micro-pillars in Fig. 10(a) depict a uniform diameter, but those in Fig. 10(b) display a non-uniform diameter. The presence of voids in Fig. 10(b) were easy to associate with bubbles that did not have enough time to spread out during the copper micro pillar reduction reaction in the MAGE process. The dependence of the internal microstructure upon the MAGE electrochemical conditions for copper micro-pillars was discussed in detail in our earlier work [17]. The strength of the electric field plays a vital role in the concentration balance of active ions (i.e., copper ions) within the local region that takes place in MAGE. We used commercial finite element analysis software (i.e., ANSYS 8.0) for simulations to establish schematic models to illustrate the development of the copper micro-pillars with different surface morphologies (as shown in Fig. 3) and internal microstructures (as depicted in Figs. 10(a) and (b)) depending upon the MAGE experimental conditions [11-12, 14-16]. Figure 10(c) shows the model in response to conditions of lower voltages but higher initial gaps (e.g., the extreme lowest case of 2.8 V with an initial gap of 15 μm), and Fig. 10(d) shows the model in response to conditions of higher voltages but lower initial gaps (e.g., the extreme highest case of 3.0 V with an initial gap of 5 μm). In other words, the model that governs the development of copper micro-pillars in the intermittent MAGE is determined by the strength and distribution of the electric field within the local region that takes place in MAGE.

The distribution of electric fields (symbolized with red arrows) in the presence of electrochemical active ions (i.e., copper ions expressed as blue dots) revealed two distinct sequential models that depend on the strength of the electric field and are shown in Figs. 10(c) and (d). Before MAGE, a sufficient amount of copper ions is present throughout the region. As soon as MAGE starts at lower voltages (i.e., at 2.8 V) with wider initial gaps (i.e., at 15 μm), the strength of the electric field is stronger in the core than at the periphery of the cylindrical zone, as shown in Fig. 10(c). This type of electric field distribution leads to the construction of a fully filled cone with a dome top that is surrounded with a halo bottom. By repeating this operation, copper micro-pillars with a smooth surface and dense internal microstructure can be fabricated, as shown in Fig. 10 (a). On the other hand, when MAGE is conducted at higher voltages (i.e., at 3.0 V) with narrow initial gaps (i.e. 5 μm), the strength of the electric field is unusually high, so it focuses on the periphery of the cylindrical zone (marginal effect), as shown in Fig. 10(d). This electric field distribution results in a deposit base established with U-shape layers. By repeating the same operation, a micro-pillar consisting of U-shape layers in the internal cross-section is obtained, as shown in Fig. 10(b). In such an unusually high electric field, numerous bubbles (caused by hydrogen evolution) are produced around the platinum microanode. Interference by the strong evolution of gas leads to a rough surface morphology outside the pillars; moreover, residues of bubbles that could not escape in time may result in void defects inside the pillars.
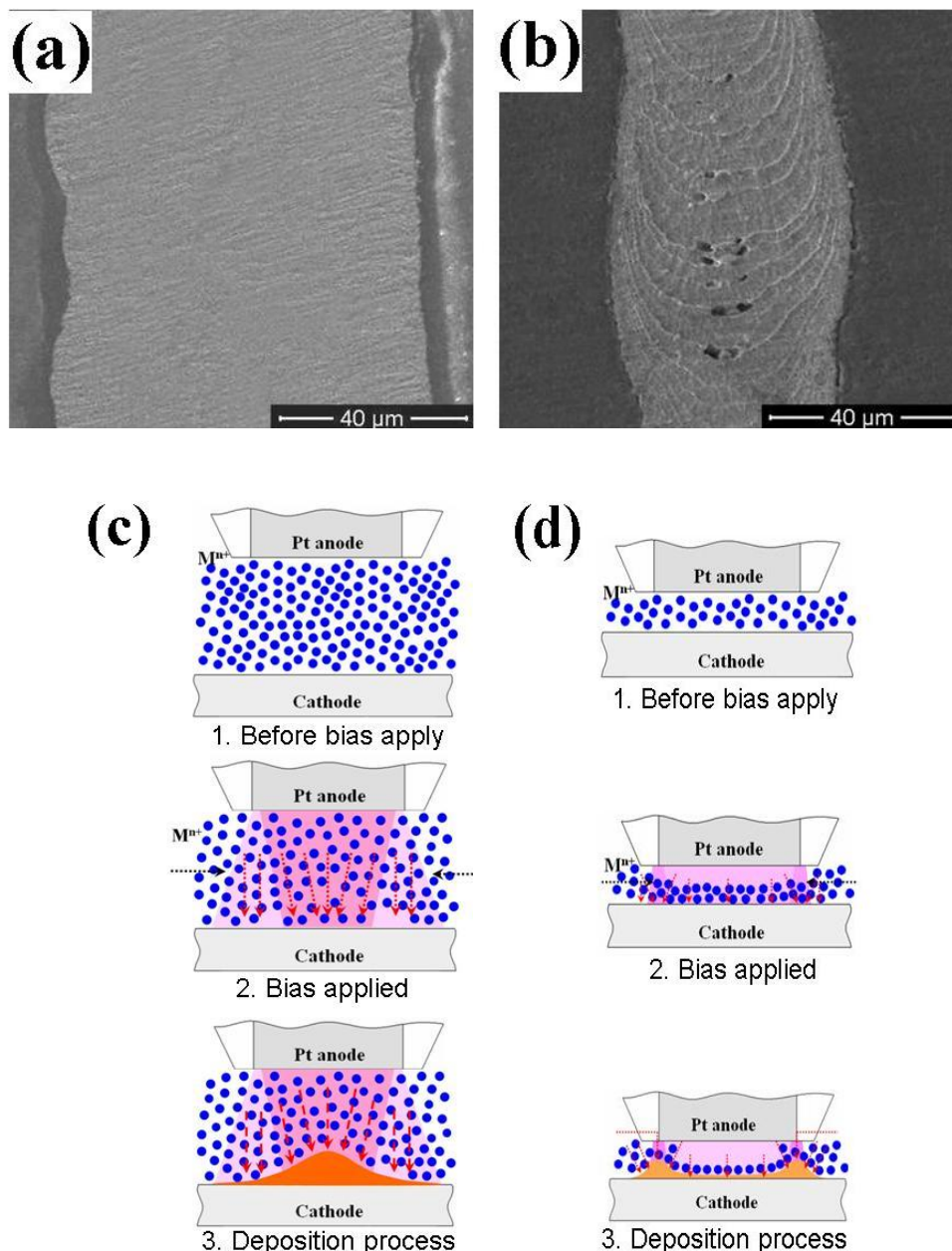
Figure 10. SEM morphology along the vertical section of the copper micro-pillars fabricated at lower electric fields (i.e., 2.8 V, 15 μm) and higher fields (i.e., 3.0 V, 5μm). (c) A schematic model proposed for the mechanism of the electrochemical deposition to form a copper micro-pillar under a high electric field by MAGE.

4.3 Proposed model for the fracture mechanism of the copper pillars

Through careful examination of the fracture SEM morphology for the copper micro-pillars, the fracture interface was found to be intimately related with the U-shape profile in the cross-sectional internal, especially when the pillars were fabricated in higher electric fields (i.e., at 3.0 V with an initial gap of 5 μm). By checking the fracture morphology around the cup-end broken part, we found that another broken part (i.e., the cone end) was removed to leave a huge cavity behind. Around the

cavity, many stripes were distributed on both sides perpendicularly to the fracture edge, as shown in Fig. 4. The micro-pillar experienced only slight necking just before fracture. The necking for micro-pillars fabricated in higher electric fields was to a lesser degree. As mentioned before, when MAGE proceeds in a very high electric field, numerous bubbles are produced within a tiny local region. Avoiding the residue of bubbles inside the pillars during their formation is inevitable. The involvement of bubble residues is more prominent when the electric field is increased during MAGE. As a result, the copper micro-pillars fabricated at higher electric fields (at 3.0 V with an initial gap of 5 μm) contain a higher density of defects. The weaker strength in mechanical properties for pillars fabricated in the high electric fields reveal may be ascribed to the higher possibility of defects present inside. Defects such as voids may provide stress concentrations that facilitate crack propagation along the interface among the conical layers (i.e., the U-shape layers in the internal cross-section depicted in Fig. 10(b). Based on the simulation models we established [17], we propose a schematic model, as shown in Fig. 11, to illustrate the fracture mechanism of the copper pillars in the testing process conducted using a nano-universal testing machine.
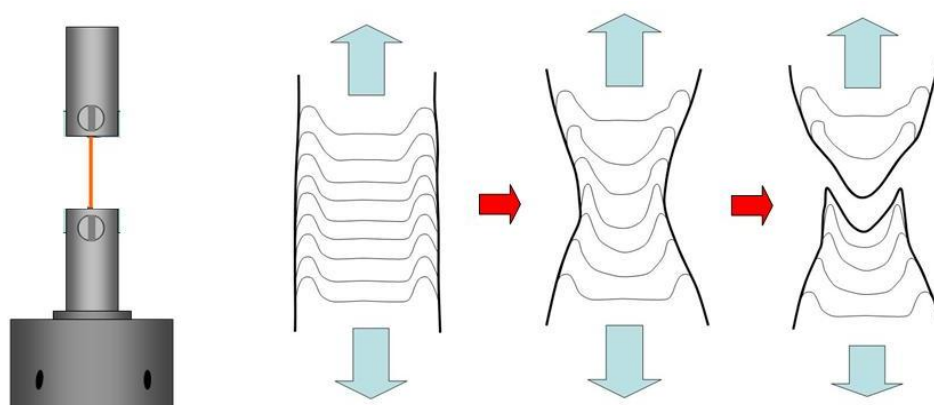

Figure 11. (a) SEM morphology of the fracture surface for the copper micro-pillar fabricated at a higher electric field (3.0 V, 5 μm). (b) A schematic model proposed to illustrate the fracture due to the micro-tensile test.

5. CONCLUSIONS

Micrometer-sized Copper pillars were prepared by the localized electrochemical deposition process (LECD) through microanode guided electroplating (MAGE) from a bath of 0.5 M copper sulfate for various electric field strengths. The mechanical properties of the micro-pillars were examined through a tensile test by means of a nano-universal testing machine. The Young's modulus, yield strength, fracture stress, and strain were estimated from the tensile testing diagrams. The surface morphology prior to and after the tensile test was examined to understand the fracture mechanics. The micro-pillars fabricated in low electric fields had a smooth surface with a dense internal microstructure. In contrast, pillars fabricated in high electric fields revealed a rough morphology and contained a higher possibility of internal defects. The mechanical properties were stronger for the

micro-pillars fabricated in a low electric field (i.e., the lowest case was 2.8 V with an initial gap of 15 μm) than those fabricated in a high electric field with a wider deposition gap (i.e., the highest case was 3.0 V with an initial gap of 5 μm). By using finite element analysis with the commercial software ANSYS 8.0, we established models for the formation development of the micro-pillars in MAGE. In this paper, we propose a model that can realize the fracture behavior of micro-pillars with distinct mechanical properties depending on the fabrication conditions in MAGE.

References

1. J. D. Madden, S. R. Lafontaine, I. W. Hunter, *Micro-Mach. Hum. Sci.*, (1995) 77.
2. J. D. Madden, I. W. Hunter, *J. Microelectromech. Syst.*, 5 (1996) 24.
3. E. M. El-Giar, U. Cairo, D. J. Thomson, *Proc. IEEE Conf. Commun. Power Comput.*, 22–3 (1997) 327.
4. E. M. El-Giar, R. A. Said, G. E. Bridges, D. J. Thomson, *J. Electrochem. Soc.*, 147 (2000) 586.
5. R. A. Said, *Nanotechnology*, 14 (2003) 523.
6. R. A. Said, *IEEE J. MEMS*, 13 (2004) 822.
7. S. K. Seol, J. M. Yi, X. Jin, C. C. Kim, J. H. Je, W. L. Tsai, P. C. Hsu, Y. Hwu, C. H. Chen, L. W. Chang, G. Margaritondo, *Electrochem. Solid-State Lett.*, 7–9 (2004) C95.
8. S. K. Seol, A. R. Pyun, Y. Hwu, G. Margaritondo, J.H. Je, *Adv. Funct. Mater.*, 15 (2005) 934.
9. S. K. Seol, J. T. Kim, J. H. Je, Y. Hwu, G. Margaritondo, *Solid-State Lett.*, 10 (2007) C44.
10. S. H. Yeo, J. H. Choo, K. S. Yip, *Proc. SPIE*, 4174 (2000) 30.
11. J. C. Lin, S. B. Jang, D. L. Lee, C. C. Chen, P. C. Yeh, T. K. Chang, J. H. Yang, *J. Micromech. Microeng.*, 15 (2005) 2405.
12. T. K. Chang, J. C. Lin, J. H. Yang, P. C. Yeh, D. L. Lee, S. B. Jiang, *J. Micromech. Microeng.*, 17 (2007) 2336.
13. J. H. Yang, J. C. Lin, T. K. Chang, G. Y. Lai, S. B. Jiang, *J. Micromech. Microeng.*, 18 (2008) 8, 055023.
14. J. C. Lin, T. K. Chang, J. H. Yang, J. H. Jeng, D. L. Lee, S. B. Jiang, *J. Micromech. Microeng.*, 19 (2009) 10, 015030.
15. J. H. Yang, J. C. Lin, T. K. Chang, X. B. You, S. B. Jiang, *J. Micromech. Microeng.*, 19 (2009) 12, 025015.
16. J. C. Lin, T. K. Chang, J. H. Yang, Y. S. Chen, C. L. Chuang, *Electrochimica Acta*, 55 (2010) 1888.
17. J. C. Lin, J. H. Yang, T. K. Chang, S. B. Jiang, *Electrochimica Acta*, 54 (2009) 5703.
18. C. S. Lin, C. Y. Lee, J. H. Yang, Y. S. Huang, *Electrochem. Solid-State Lett.* (2005) C125.